Supplementary Material :

APPENDIX A:

Table A1: Parameters of the model and baseline values used in numerical simulations

Parameter	Description	Values
β	Encountering rate between active males and available females	3
d	Basal death rate	0.1
δ_e	Mate searching energetic cost for all individuals	0.1
δc	Competition cost in active males	0, 0.01, 0.02, …, 1
δ□	Egg laying cost in mated females	0.1
p	Maximum number of partners per female	1, 2, 3, 4, 5
b	Mean offspring number per female per day	5
e	Emergence peak time	0.1, 0.2, …, 0.8, 0.9
v_e	Variance in the timing of emergence	0.01, 0.02, …, 0.15
μ	Mutation size of the reproductive activity period timing	0.04
B	Number of neutral loci in the neutral genome	10
μ_G	Mutation rate of each neutral loci	0.1
G	Genetic threshold of reproductive isolation	0.1, 0.2, …, 0.8, 0.9, 1
K	Carrying capacity of the environment	1000, 2000, 5000

Table A2: Individual Attributes

Attribute	Description	Values
sex	Sex of the individual	"M" or "F"
h_a	Center of the reproductive activity period	$0 \leq h_a \leq 1$
w_a	Range of the reproductive activity period	0.15
f	Female fertilization status	0 or 1
p_n	Current number of mating attempts by a female	$0 \leq p_n \leq p$
E	Number of eggs laid by a mated female	Variable positive integer

Supplementary Material and Methods

Each of our individually-centered simulations considered a series of consecutive days within which different stochastic events may happen, with different probabilities defined further in the appendix. Each day (a continuous interval from sunrise (t = 0) to sunset (t = 1)) was split into smaller time intervals . These intervals are defined by the temporal position of *known* stochastic events, drawn each day.

- *Known* events are changes in the state of the population that depend solely on the traits of the individuals alive at dawn, i.e. the transitions from resting to reproductive activity (and *vice versa*) for every individual, as well as the emergence of new adult individuals. The number of known events is thus at least 2*Number of individuals + Number of emerging individuals.

A second type of stochastic event can happen between two *known* events, which are *unknown* events.

- *Unknown* events are changes in the state of the population that depend on interactions between individuals and whose occurrence cannot be known by looking at individual traits alone. These are *mating* and *death* events. The individual involved in an event is randomly chosen, uniformly among individuals exhibiting the same status. The time at which the next event happens is drawn in an exponential distribution, based on the current numbers of active males $\mathbf{N_a}^{\male}$, resting males $\mathbf{N_r}^{\male}$, available active females $\mathbf{N_a}^{\female}$, resting available females $\mathbf{N_r}^{\female}$, and unavailable females $\mathbf{N_m}^{\female}$. We continue drawing new mating or death events until the drawn time exceeds the time of the next known event. At that point, a new individual emerges or an individual exchanges resting and active statuses, and thus modifies the rate of occurrence of mating and death events. Hence the known event is prioritized and takes place, and it modifies occurrence rates of unknown events accordingly.

Unknown events occurrence times and rates are computed using the instantaneous mating rate λ_r and the instantaneous death rate λ_d, given by:

(1)

$$\lambda_r = \beta * N_a^{\female} * N_a^{\male}$$

(2)

$$\lambda_d = d * (N_a^{\male} + N_r^{\male} + N_a^{\female} + N_r^{\female} + N_m^{\female}) + \delta_e * (N_a^{\male} + N_a^{\female}) + \delta_c * N_a^{\male} * (N_a^{\male}-1) + \delta_l * \sum_{i=0}^{N_m^{\female}} E_i$$

The time at which those events happen is drawn in an exponential distribution of parameter $\lambda r + \lambda d$. If this occurring time is smaller than the occurring time of the next known event, then a mating or a death event happens. If this occurring time is higher than the occurring time of the next known event, nothing happens except the next known event. To determine which event between mating and death occurs, a value is drawn from a uniform distribution $U(0,1)$ and is compared to $\frac{\lambda r}{\lambda r+\lambda d}$. If the value drawn is smaller, then a mating event occurs. If not, we compare it with $\frac{\lambda r}{\lambda r+\lambda d} + \frac{d^* N_r^{\male}}{\lambda r+\lambda d}$, which corresponds to the death of an inactive male. If the value is still greater, we compare with $\frac{\lambda r}{\lambda r+\lambda d}. + \frac{d^* N_r^{\male}}{\lambda r+\lambda d} + \frac{(d+\delta_e)^* N_a^{\female}}{\lambda r+\lambda d}$ (death of an available active female), and so on.

In the case of unavailable females, we consider the number of eggs E_i laid by each individual.

As such, there are $\mathbf{N_m}^{\female}$ events we need to check:

We compare the value drawn from the uniform distribution to with to:

- $\frac{\lambda r}{\lambda r+\lambda d} + \ldots + \frac{d+\delta_l * E_1}{\lambda r+\lambda d}$ for the death of unavailable female number 1;
- $\frac{\lambda r}{\lambda r+\lambda d} + \ldots + \frac{2d+\delta_l *(E_1+E_2)}{\lambda r+\lambda d}$ for the death of unavailable females number 2;

and so on until the event of the death of unavailable female number $\mathbf{N_m}^{\female}$:

- $\frac{\lambda r}{\lambda r+\lambda d} + \ldots + \frac{(N_m^{\female} * d)+\delta l * \sum_{i=1}^{N_m^{\female}} E_i}{\lambda r+\lambda d}$.

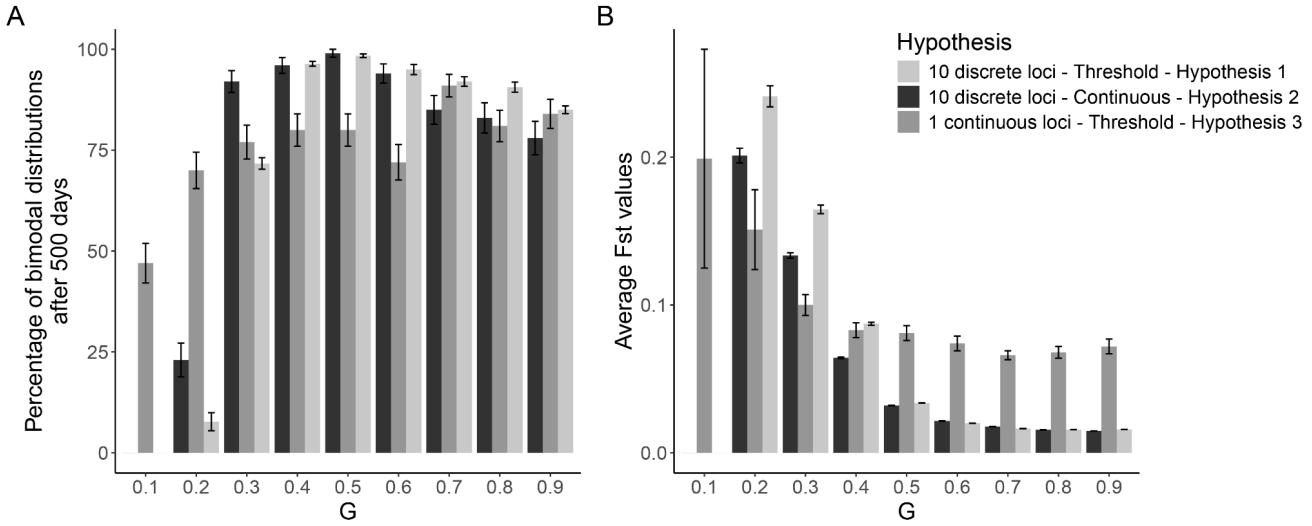

Figure S1: **Effect of the proportion of loci *G* on population differentiation depending on three different hypotheses on the link between the divergence at the neutral loci and incompatibility between mating partners.** We compared the different outcomes obtained assuming these three different hypotheses (described below), and showed them in varying shades of gray**.** 100 simulations were run for each hypothesis. We characterised either (A) the percentage of simulation ending in a bimodal distribution of the reproductive activity timing and (B) the average *Fst* values between the two sub-populations. The three hypotheses assumed are described as :

- **Hypothesis 1** assumes 10 neutral loci underlying incompatibilities and a threshold effect represented by the value *G*. This hypothesis implies a discrete effect of incompatibility alleles : when two mating partners have more than a proportion *G* of differences at their 10 neutral loci, they can not reproduce at all. This assumption is used for all the simulations shown in the main manuscript.
- **Hypothesis 2** assumes a continuous effect of incompatibility alleles at 10 neutral loci**.** The mean number of offspring (N_{off}) produced by a pair of mates with a difference N_{dist} between their neutral loci is determined by a logistic function, so that $N_{off} = 1 - \left(\frac{1}{1+e^{(-20*(Ndist-G))}}\right)$.
- **Hypothesis 3** assumes a single neutral loci with a continuous value, and a threshold effect *G*, similar to hypothesis 1.

We observe qualitatively similar results for all three hypotheses on the effect of neutral loci on incompatibilities between mating partners, with slight differences in F_{st} values: the threshold hypothesis 1 leads to higher F_{st} compared to the hypothesis 2, while the hypothesis 3 led to higher F_{st} values for higher *G* values.
Error bars show the SD computed over the 100 replicates per value of *G*. All simulations were run assuming the same values in the other parameters: $\delta_c = 0.1$, $\beta = 3$, $e = 0.5$, $v_e = 0.05$, $p = 1$, K=1000.

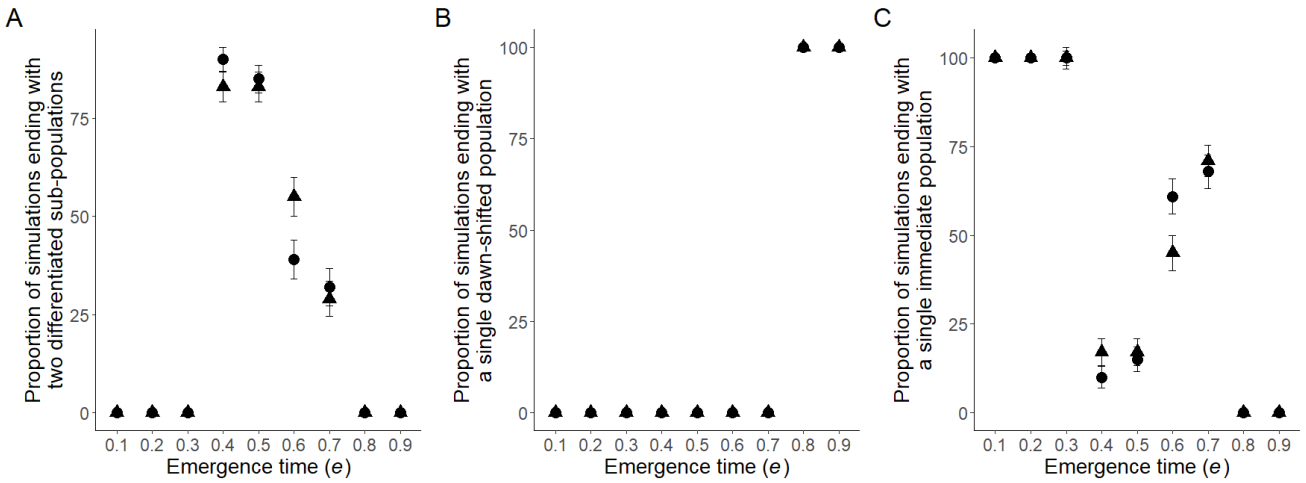

Figure S2: **Effect of the duration of simulations on the evolutionary outcomes observed.** Circles and triangles indicate simulation outcomes after 500 and 2000 days respectively. We ran 100 simulations per condition, and distinguished them based on the distribution of the timing of reproductive activity h_a after 500 days. These distributions observed at the end of the simulation showed either the coexistence of two sub-populations (*immediate* and *dawn-shifted*) (A), a single *dawn-shifte*d population (B) or a single *immediate* population (C). We observe similar patterns no matter the simulation length, we thus used 500-days outcomes for all analyses in this study.
Error bars show the standard deviation of the proportions observed in the 100 replicated simulations. All simulations were run assuming the same parameter values: $\delta_c = 0.1$, $\beta = 3$, $G = 1$, $v_e = 0.05$, $p = 1$, K=1000.

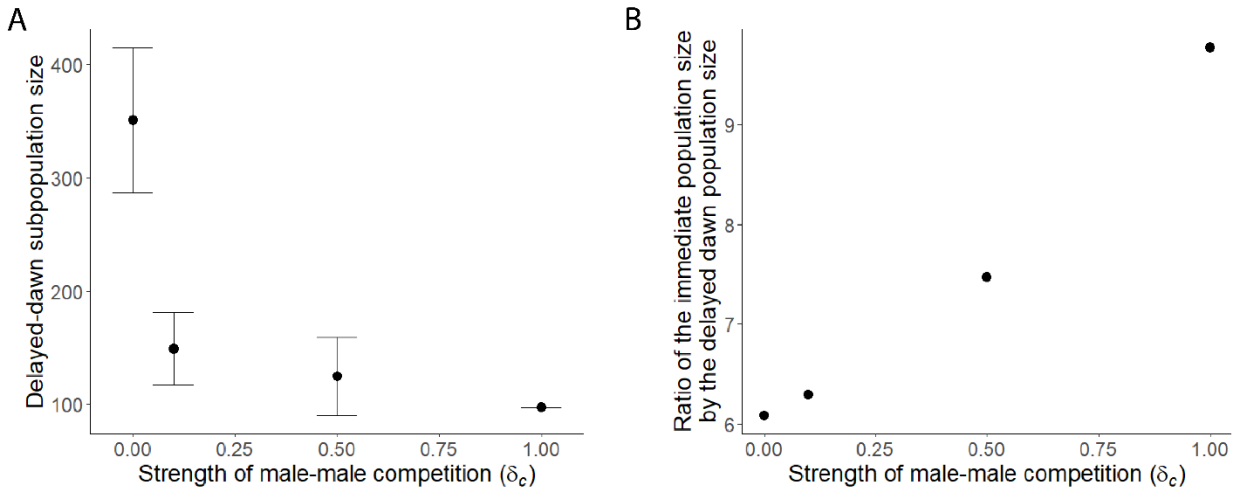

Figure S3: **Effect of male-male competition (δ_c) on the size of the *delayed-dawn* subpopulations.** We run 100 simulations per parameter. We characterized *delayed-dawn* sub-populations either by (A) their population size or (B) the ratio between the size of the *delayed-dawn* subpopulation and the *immediate* sub-population. We observe that higher male-male competition values lead to a smaller size in the *delayed-dawn* while the *immediate* sub-population maintains a similar size for higher values of δ_c (average *immediate* population size for $\delta_c = 0.1$ and $\delta_c = 1$ are 938.73 and 948 respectively, with no significant difference) .This difference in sub-population sizes explains the higher risk of extinction of *dawn-shifted* sub-populations within our simulations.
Error bars show the SD computed over the 100 replicates per value of δc. All simulations were run assuming the same values in the other parameters: $\beta = 3$, $G = 1$, $e = 0.5$, $v_e = 0.05$, $p = 1$, K=1000.

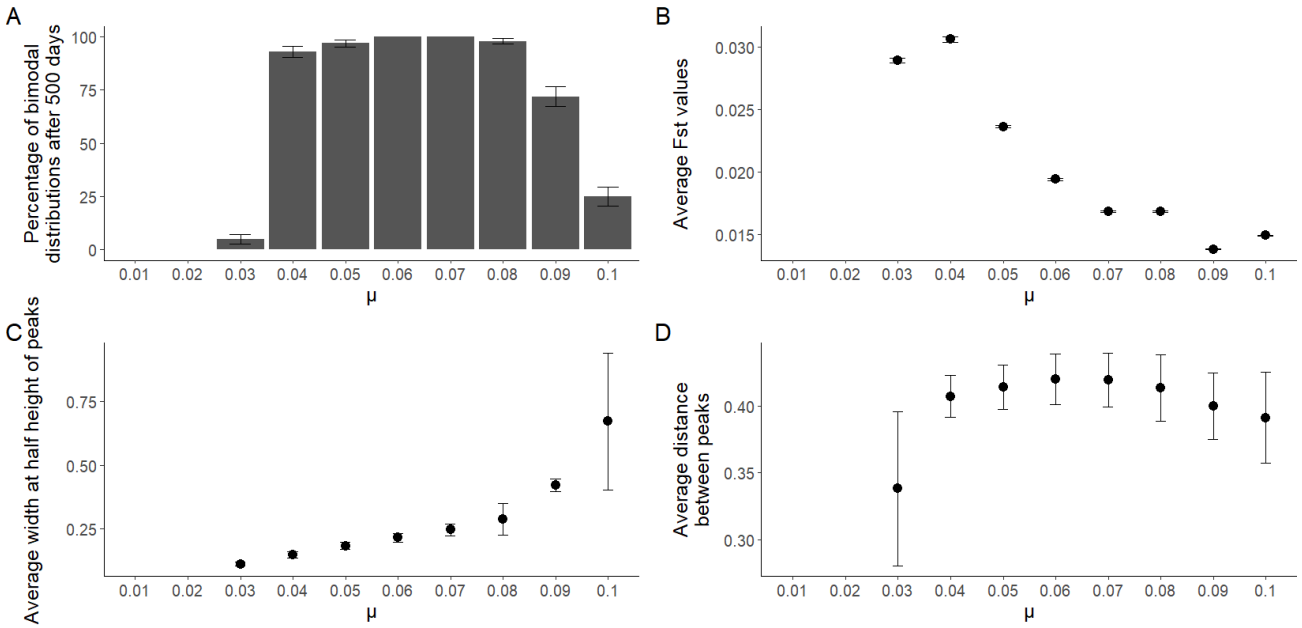

Figure S4: **Effect of the mutation effect μ on the evolution of differentiated sub-populations in a *daily* model,** depending on the proportion of loci necessary to generate incompatibilities G. Characterisation of the results of 100 simulations per parameter is presented above with (A) the percentage of bimodal distributions after 500 days. (B) The average F_{st} between sub-populations after 500 days. (C) The average width at half height of the peaks in the distribution of the reproductive activity timing, as well as (D) the average distance between the two peaks in reproductive activity timing. We can observe that low values of μ tend to not allow for differentiation within the population to occur, while high values disrupt the population structure, making inheritance of the activity time too random. The spread in activity timing becomes very large, and F_{st} values drop significantly. Medium values on the other hand, allow for temporal differentiation between sub-populations.
Error bars show the SD computed over the 100 replicates per value of μ. All simulations were run assuming the same values in the other parameters: $\delta_c = 0$ .1, $\beta = 3$, $G = 1$, $e = 0.5$, $v_e = 0.05$, $p = 1$, K=1000.

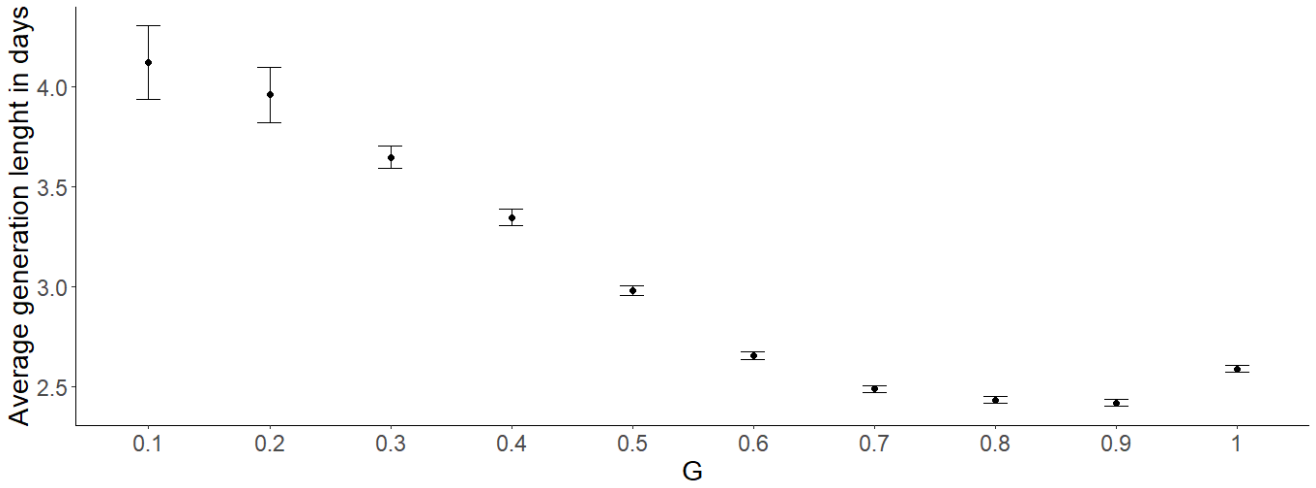

Figure S5: **Average generation time within simulation, depending on the proportion of loci necessary to generate incompatibilities *G*.** We run 100 simulations per parameter, measuring the average length of a generation. Generation time is lowered as *G* rises, from 4 days to only 2.5.
Error bars show the SD computed over the 100 replicates per value of δ_c. All simulations were run assuming the same values in the other parameters: $\delta_c = 0.1$, $\beta = 3$, $e = 0.5$, $v_e = 0.05$, $p = 1$, K=1000.

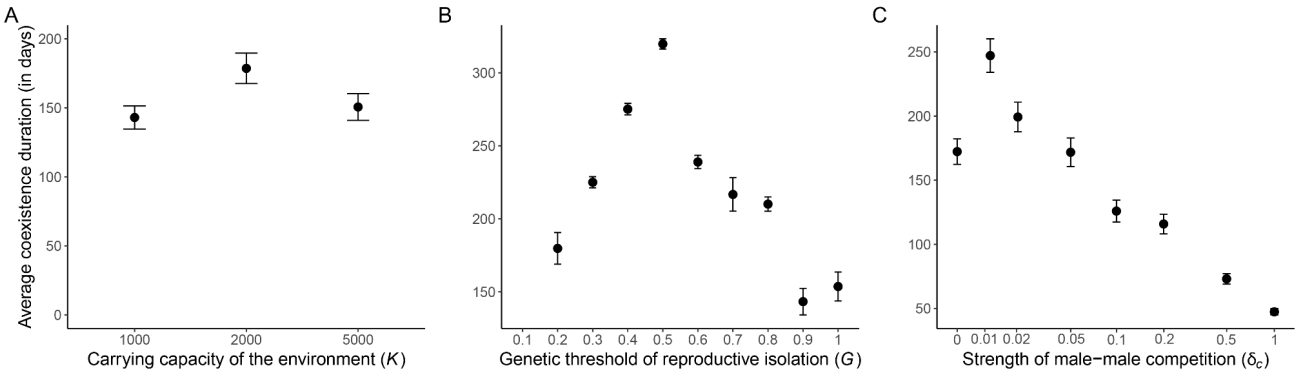

Figure S6: **Factors shaping the duration of coexistence between *dawn-shifted* and *immediate* sub-populations.** We ran 100 simulations for 500 days and followed the duration of coexistence between *dawn-shifted* and *immediate* sub-populations, depending on different parameters: (A) The carrying capacity K. (B) The genetic threshold G of reproductive isolation. (C) The strength of male-male competition δ_c.

Error bars show the SD computed over the 100 replicates per value of the parameters. All simulations were run assuming the same values in the other parameters: $\delta_c = 0.1$, except in fig. 14C, $\beta = 3$, $G = 1$, except in fig. 14B, $e = 0.5$, $v_e = 0.05$, $p = 1$, K=1000, except in fig. 14A.

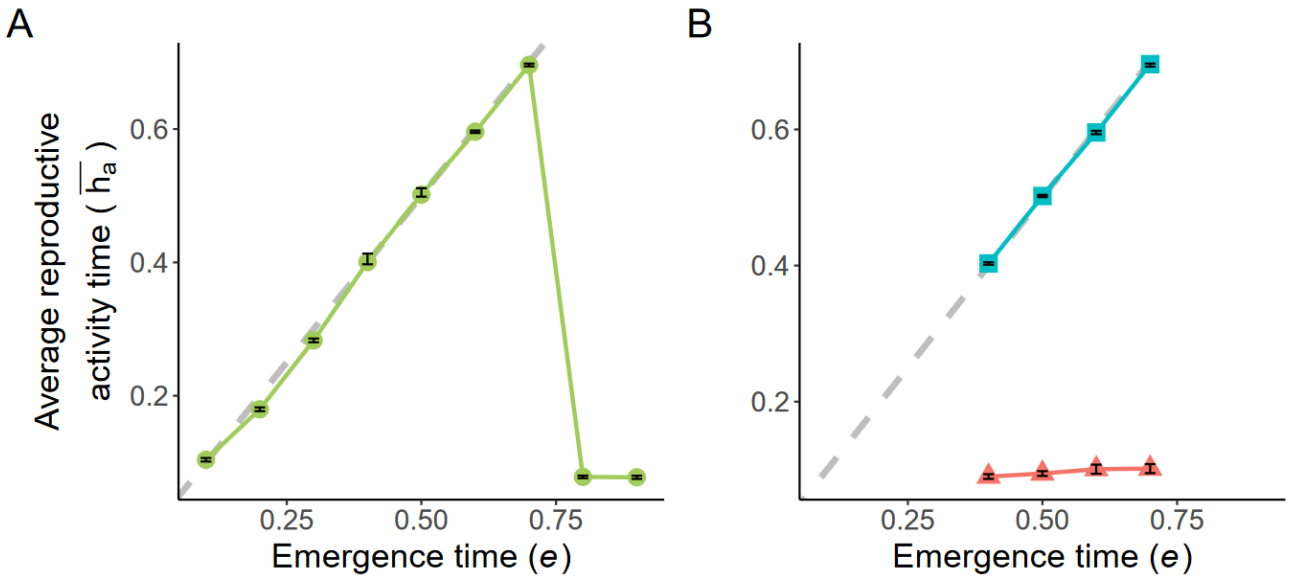

Figure S7: **Effect of the timing of adult emergence (*e*) on the temporal niches occupied by the different sub-populations**, estimated by the average reproductive activity timing (h_a) within sub-populations. We ran 100 simulations per value of the emergence time e for 500 days. These distributions observed at the end of each simulation were either unimodal (A) or a bimodal (B). When simulations led to bimodal distribution, *dawn-shifted* and *immediate* temporal niches were observed, and the average h_a within each of the two sub-populations are shown in red triangles and blue squares respectively. Dashed lines then show the emergence time e in the corresponding simulations, to better visualize the match with the surge of freshly emerged females.
Error bars represented by the SD computed over the 100 replicates per value of e. All simulations were run assuming the same values for the other parameters: $\delta_c = 0.1$, $\beta = 3$, $G = 1$, $v_e = 0.05$, $p = 1$, K=1000.

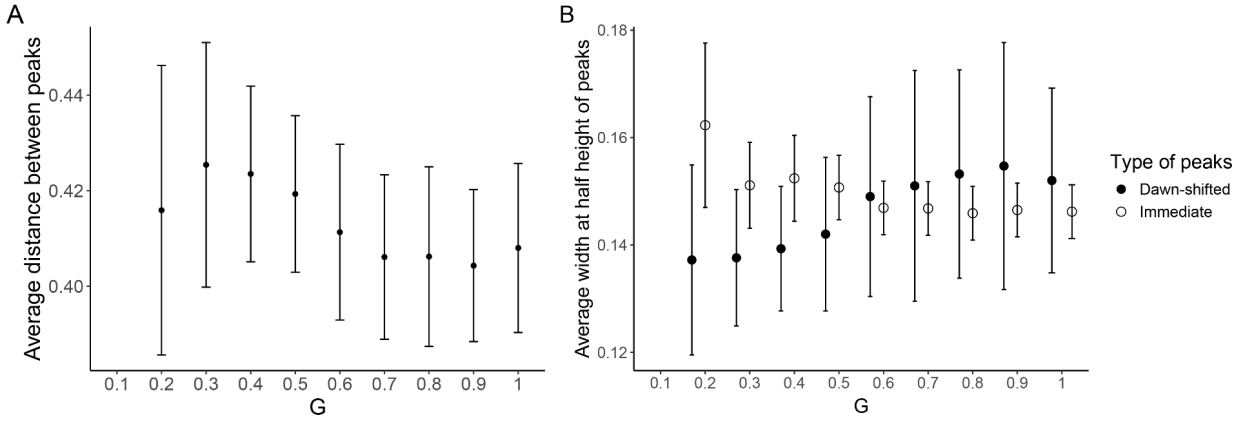

Figure S8: **Characterization of the temporal niches occupied by different subpopulations, using the distribution of timing of activity values (h_a) observed at the end of the simulations. The** average distance between the peaks (A) observed in bimodal distributions, as well as the average width of the peaks depending on their type (B), all depending on the proportion of loci necessary to generate incompatibilities (G) are shown. We run 100 simulations for each parameter.This characterization shows that the two sub-populations observed in the simulations with a bimodal distribution detected indeed had limited temporal overlap, and are thus actually temporally segregated. For lower values of G, smaller peak widths might be caused by a smaller population size due to the stricter threshold allowing successful reproduction.

Error bars show the SD computed over the 100 replicates per value of G. All simulations were run assuming the same values in the other parameters: $\delta_c = 0.1$, $\beta = 3$, $e = 0.5$, $v_e = 0.05$, $p = 1$, K=1000.

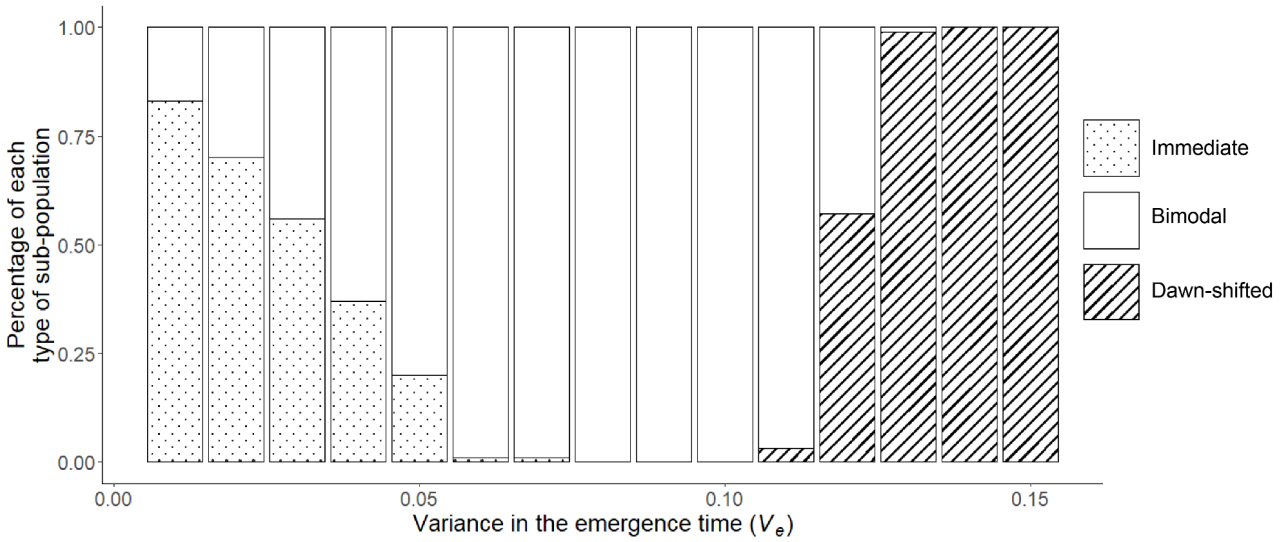

Figure S9: **Effect of variance in the timing of adult emergence (v_e) on the evolution of sub-populations with differentiated temporal niches**. The percentage of simulations where either one or two sub-populations were observed after 500 days is shown, for 100 replicates per value of the variance in the timing of adult emergence v_e, assuming that this timing of emergence is centered around noon ($e = 0.5$). When only a single population was maintained, we distinguish *dawn-shifted* (in stripes) and *immediate* (in dots) populations. Simulations may also result in the coexistence of two sub-populations, with *bimodal* (in white) timing of reproductive activities. All simulations were run assuming the same values in the other parameters: $\delta_c = 0.1$, $\beta = 3$, $G = 1$, $e = 0.5$, $p = 1$, K=1000.

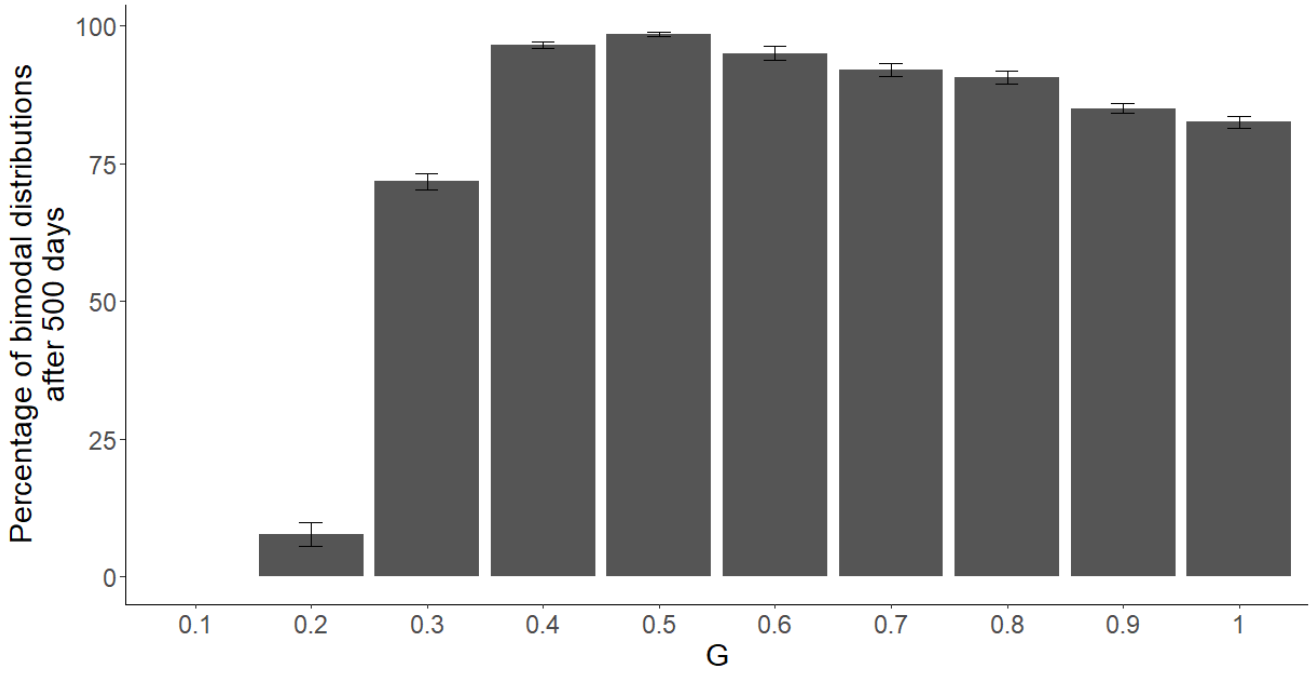

Figure S10: **Effect of the proportion of loci *G* required to generate incompatibility between mates on the evolution of sub-populations with different temporal niches.** The percentage of simulations where a bimodal distribution in the timing of activities is observed at 500 days, depending on the proportion of loci *G* necessary to trigger incompatibility.
Error bars are the SD computed over the 100 replicates per value of *G*. All simulations were run assuming the same values in the other parameters: $\delta_c = 0.1$, $\beta = 3$, $e = 0.5$, $v_e = 0.05$, $p = 1$, K=1000.

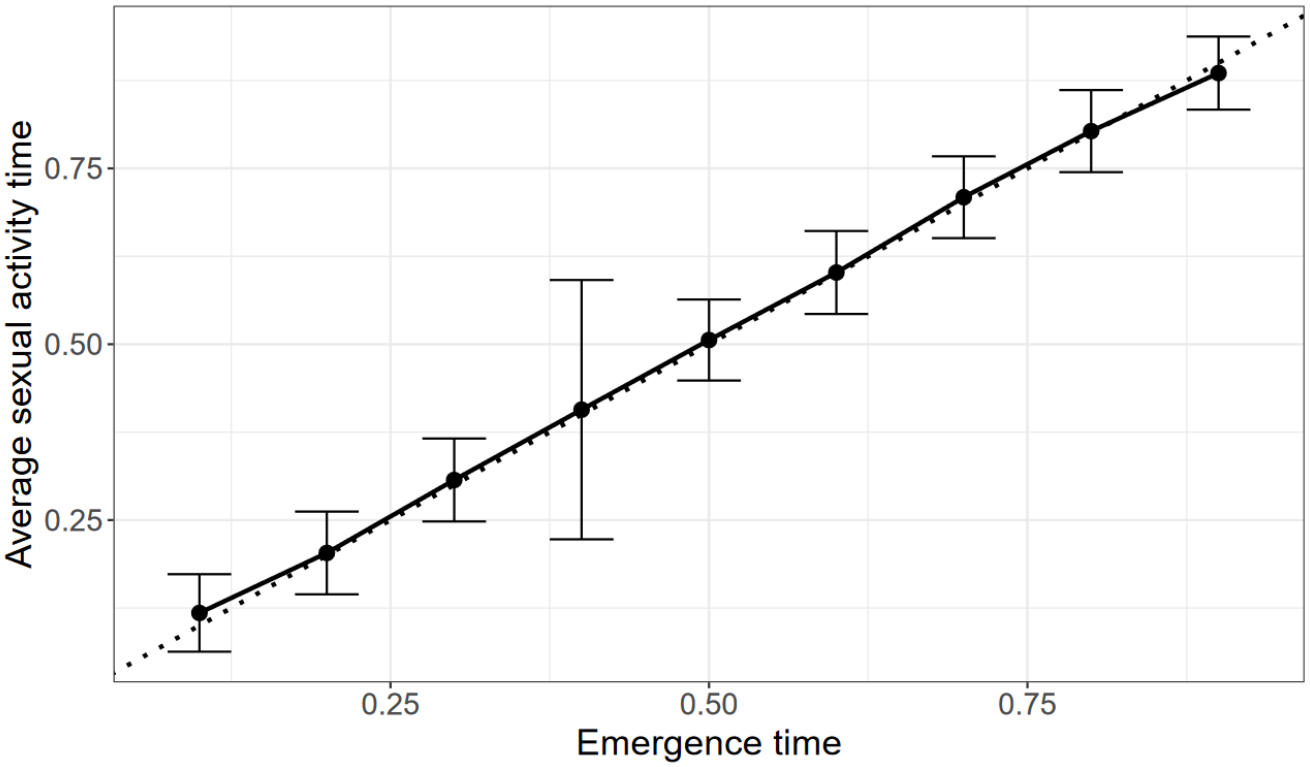

Figure S11: **Effect of the emergence time *e* on the average timing of reproductive activities in a *seasonal* model (*i.e.* assuming non-overlapping generations).** The dotted line shows the emergence timing (*e*). In the seasonal model, average activity times are centered around the time of emergence, and no bimodality is observed in the timing of reproductive activities, assuming low level of male-male competition.
Error bars are 95% confidence intervals computed over the 100 replicates per value of *e*. All simulations were run assuming the same values for the other parameters: $\delta_c = 0.1$, $\beta = 3$, $G = 0.4$, $v_e = 0.05$, $p = 1$, $K=1000$.

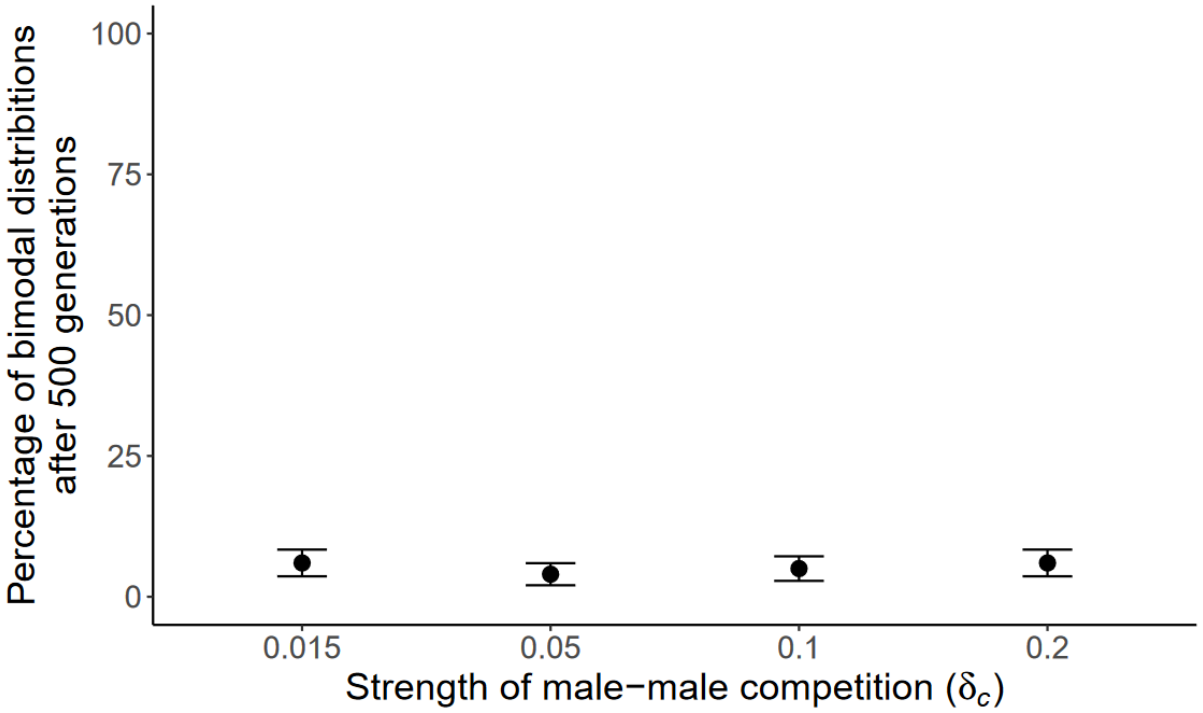

Figure S12: **Effect of limited cost of male-male competition (δ_c) on the emergence of bimodal distribution in the activity time, in a *seasonal* model.** We can observe that male-male competition values generating bimodal distribution of reproductive activities on the daily model (see Figure 4A) barely produces any bimodal distribution in the activity timings in the seasonal model. Evolution of differentiated temporal niches indeed only happened in circa 5% of the simulations.
Error bars show the SD computed over the 100 replicates per value of δ_c. All simulations were run assuming the same values in the other parameters: $\beta = 3$, $G = 0.4$, $e = 0.5$, $v_e = 0.05$, $p = 1$, K=1000.

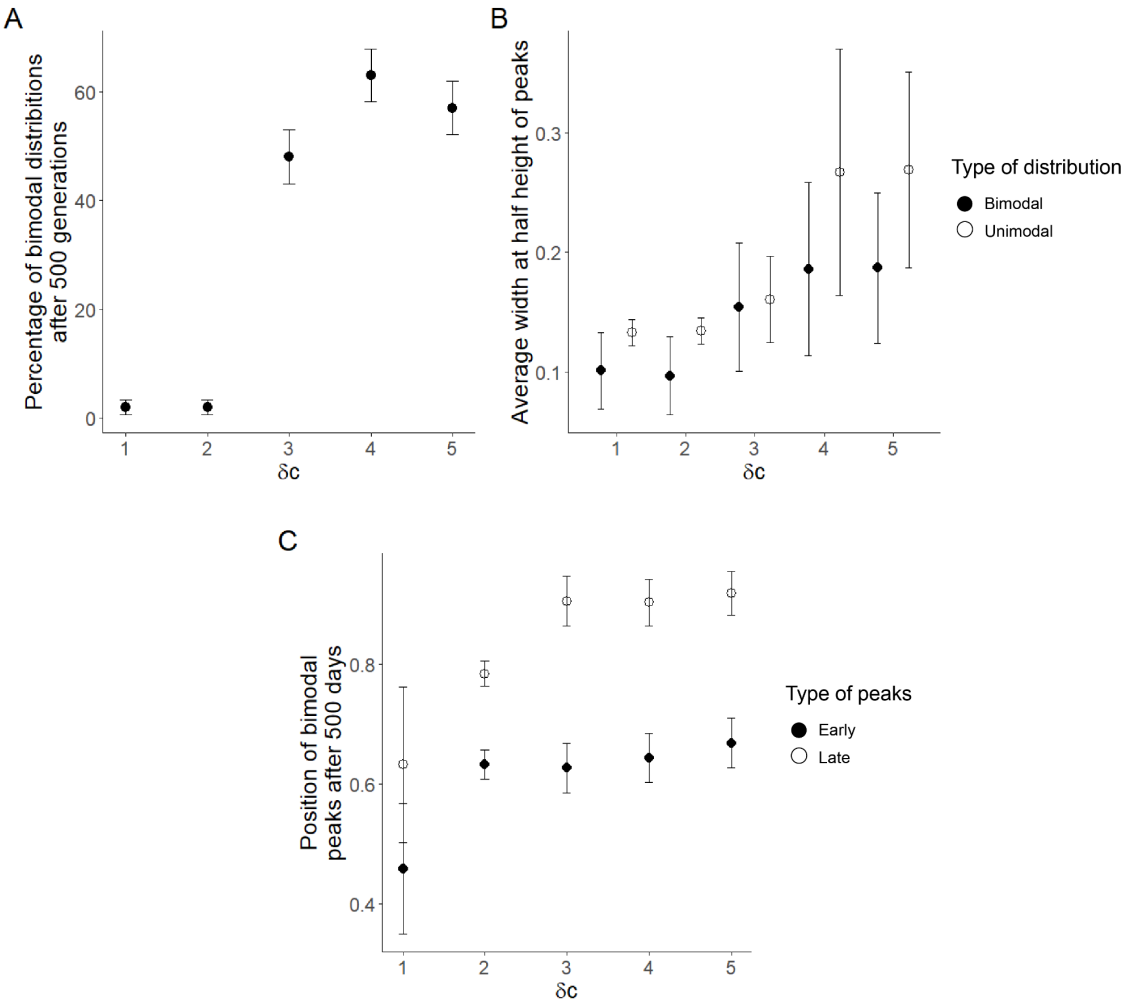

Figure S13: **Effect of the cost of male-male competition (δ_c) on the evolution of differentiated sub-populations in a *seasonal* model**. We ran 100 simulations per δ_c value, and distinguished the observed evolutionary outcome based on the distribution of the timing of reproductive activity h_a after 500 days. (A) Percentage of differentiated populations observed depending on the cost of male-male competition δ_c. High male-male competition can still produce frequent bimodality in the activity timings in a seasonal model, but only for extreme values of δ_c. (B) Average width at half height of the peaks in reproductive activity timing, depending on the type of distribution (either unimodal or bimodal). We can observe that the spread in activity timing is usually larger when only one peak is present, rather than two. Higher cost for male-male competitions also correlates with wider peaks and thus larger windows of activity within a sub-population. (C) Temporal positions of sub-populations when two were observed, depending on the cost of male-male competition δ_c. We can observe that higher cost for male-male competition is correlated with later and later timings of reproductive activity for those sub-populations, especially for the late one.
Error bars show the SD computed over the 100 replicates per value of δc. All simulations were run assuming the same values in the other parameters: $\beta = 3$, $G = 0.4$, $e = 0.5$, $v_e = 0.05$, $p = 1$, K=1000.

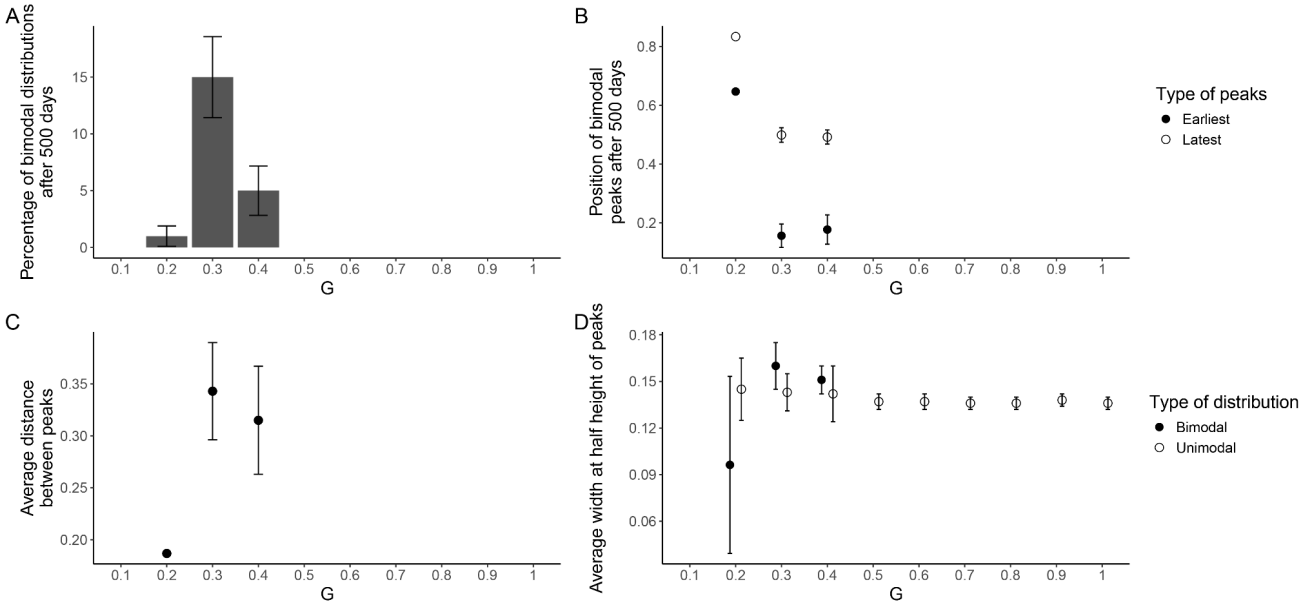

Figure S14: **Investigating the effect of independent genetic control of reproductive activity timing in males and females in the daily model.** Characterisation of the results of 100 simulations per parameter assuming sex-specific timing of reproductive activity are presented above with (A) the percentage of bimodal distributions after 500 days. (B) The position of peaks in reproductive activity timing, in simulations ending with a bimodal distribution of the h_a trait. (C) The average distance between the two peaks in reproductive activity timing, as well as (D) the average width at half height of those peaks, depending on the type of distribution. We can observe that only a narrow set of values of G allow for population differentiation, and that most sub-populations did not exhibit overlap with one another (except when G=2).

Error bars show the SD computed over the 100 replicates per value of G. All simulations were run assuming the same values in the other parameters: $\delta_c = 0$ .1, $\beta = 3$, $e = 0.5$, $v_e = 0.05$, $p = 1$, K=1000.

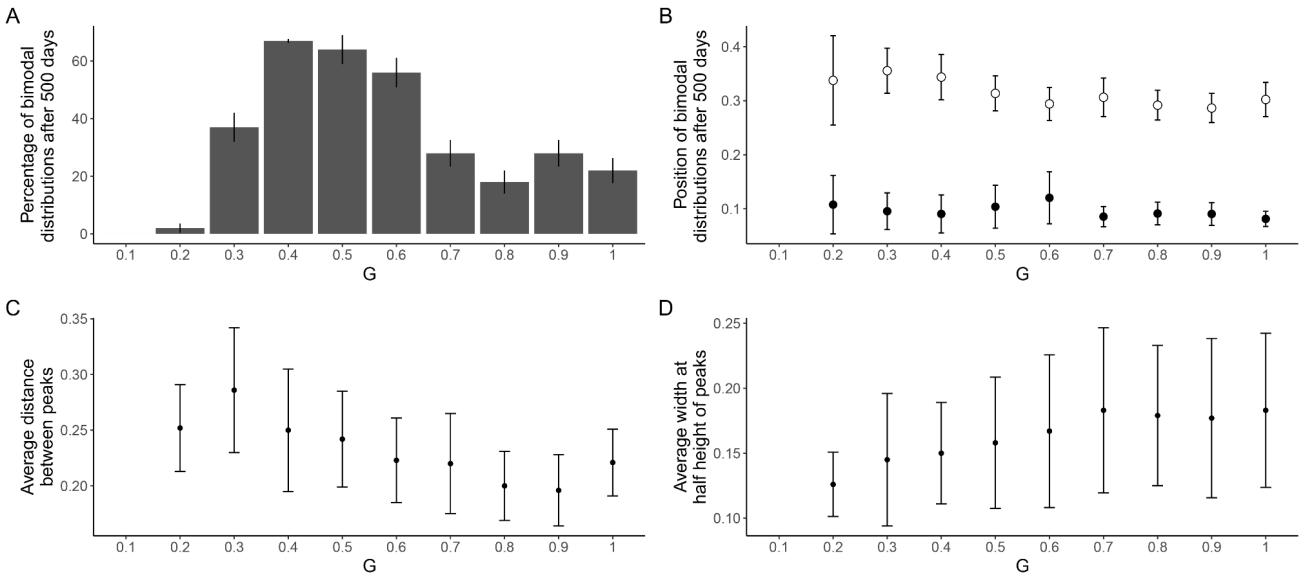

Figure S15: **Effect of the coevolution of sexual activity timings (h_a) and emergence timing (*e*) on the evolution of differentiated sub-populations in the *daily* model,** depending on the proportion of loci *G* necessary to generate incompatibilities. Characterisation of the results of 100 simulations per parameter with coevolution of h_a and *e* are presented above with (A) the percentage of bimodal distributions after 500 days. (B) The position of peaks in reproductive activity timing, in simulations ending with a bimodal distribution of the h_a trait. (C) The average distance between the two peaks in reproductive activity timing, as well as (D) the average width at half height of those peaks. We observed differentiation when the coevolution of h_a and *e* was allowed, albeit at a lower frequency than when *e* was fixed. Both sub-populations seem to display early activity, with limited overlap in reproductive activity timing.
Error bars show the SD computed over the 100 replicates per value of *G*. All simulations were run assuming the same values in the other parameters: $\delta_c = 0.1$, $\beta = 3$, $e = 0.5$, $v_e = 0.05$, $p = 1$, K=1000.